Giant Magneto-Optical Faraday Effect in HgTe Thin Films in the Terahertz Spectral Range

A. M. Shuvaev,[1] G. V. Astakhov,[2,*] A. Pimenov,[1] C. Brüne,[2] H. Buhmann,[2] and L. W. Molenkamp[2]

[1]*Institute of Solid State Physics, Vienna University of Technology, 1040 Vienna, Austria*
[2]*Physikalisches Institut (EP3), Universität Würzburg, 97074 Würzburg, Germany*

(Received 8 November 2010; published 11 March 2011)

We report the observation of a giant Faraday effect, using terahertz (THz) spectroscopy on epitaxial HgTe thin films at room temperature. The effect is caused by the combination of the unique band structure and the very high electron mobility of HgTe. Our observations suggest that HgTe is a high-potential material for applications as optical isolator and modulator in the THz spectral range.

DOI: 10.1103/PhysRevLett.106.107404 PACS numbers: 78.20.Ls, 78.20.Ek, 78.66.Hf

The extreme purity of thin film semiconductors and semimetals available today provides very high mobility and mean-free paths of the charge carries. In HgTe, which has a so-called inverted band structure, this has lead to the observation of a number of fascinating spin and transport phenomena [1–3]. Here we show that highly mobile electrons in HgTe films also result in a giant room temperature Faraday rotation at terahertz (THz) frequencies. In a 70 nm-thick HgTe layer the Verdet constant—i.e., the Faraday rotation normalized by magnetic field strength and layer thickness—is as large as 10^6 rad T^{-1} m^{-1}. This is orders of magnitudes larger than the record values in terbium gallium garnet (10^2 rad T^{-1} m^{-1}) [4], the diluted magnetic semiconductor (Cd,Mn)Te (10^3 rad T^{-1} m^{-1}) [5], and the narrow-gap semiconductor InSb (10^4 rad T^{-1} m^{-1}) [6].

The optical properties of semiconductors and semimetals at terahertz (THz) frequencies are determined by the free-carrier response. The oscillating electric field $E_y e^{-i\omega t}$ of the THz radiation accelerates the free carriers and thus generates an alternating current (ac) in the material. In a constant external magnetic field B, moving carriers experience the Lorentz force acting perpendicular to their direction of motion. Owing to this ac Hall effect, the oscillating current generates THz radiation polarized perpendicular to the primary polarization; i.e., a component $E_x e^{-i\omega t}$ appears in the system's response [Fig. 1(a)]. The resulting Faraday rotation of the transmitted radiation can, in the limit $E_x \ll E_y$ and in the low frequency approximation, be written as [6]

$$\theta \cong \frac{Z_0}{2\sqrt{\varepsilon}} L\sigma_{xy}(\omega). \quad (1)$$

Here, $Z_0 \simeq 377\ \Omega$ is the impedance of the vacuum and ε and L are the dielectric constant and the thickness of the sample, respectively. In low magnetic fields, the dc Hall conductivity is $\sigma_{xy}(0) = \sigma_0 \mu B/c$. Here σ_0 is the dc conductivity, μ is the mobility, and c is the speed of light.

The strength of the Faraday rotation in a material is characterized by the Verdet constant $\mathcal{V} \equiv \theta/BL \propto \mu^2 N$. Intrinsic semiconductors often have a high mobility $\mu = e\tau/m$ because of the low scattering rate τ^{-1}, which is limited only by phonon scattering. However, because of the finite band gap, the intrinsic carrier concentration N is rather low, even at room temperature (RT), and the Verdet constant is small. From this perspective, the zero-gap material HgTe—which is in addition characterized by a small effective mass ($m = 0.035 m_0$)—is an attractive material to obtain a giant Faraday effect.

The results in this Letter have been obtained using quasioptical terahertz spectroscopy [7,8] in transmittance geometry. Our THz spectrometer utilizes linearly polarized monochromatic radiation in the frequency range from 0.1 THz to 0.9 THz (from 0.4 meV to 3.7 meV) which is provided by backward-wave oscillators. An opto-acoustic Golay cell or a He-cooled bolometer is used as a detector of

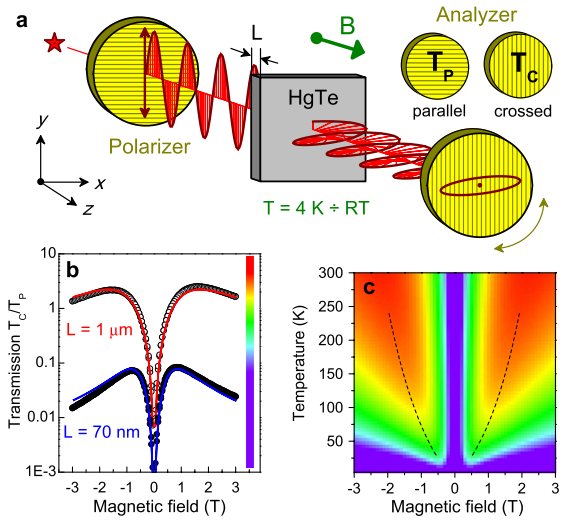

FIG. 1 (color online). *THz Faraday effect in HgTe.* (a) Detection of the transmission energy in crossed (T_C) and parallel (T_P) configurations of the polarizer and analyzer. (b) Ratio T_C/T_P in HgTe of thicknesses $L = 1$ μm and $L =$ 70 nm obtained at $T = 200$ K for a frequency $\omega = 0.35$ THz (symbols). The lines correspond to the model calculation (see text for details). (c) Temperature evolution of $T_C/T_P(B)$ in HgTe with $L = 1$ μm. For this calculation the experimental temperature dependencies of m, N, and μ [see insets of Fig. 3] are used.

the radiation. In order to measure the polarization of the radiation we use wire grid polarizers. The amplitude $|t|$ and the phase shift ϕ of the radiation transmitted through the sample are then measured by using a Mach-Zehnder interferometer arrangement [9].

Here, we present results for two samples, 70 nm-thick and 1 μm-thick HgTe layers (nominally undoped), grown by molecular beam epitaxy on an insulating CdTe substrate [10]. For our experiments we use a straightforward apparatus layout with a fixed polarizer and a rotating analyzer, allowing us to measure the power density of the THz radiation that is transmitted by the HgTe samples in cross T_C and parallel T_P polarizer configurations [Fig. 1(a)]. Typical data on the dependence of T_C/T_P on the magnetic field for both samples are shown in Fig. 1(b). We observe that at the maximum of the curve for the thick sample ($L = 1$ μm), $T_C > T_P$, implying an unusually large Faraday rotation. From $\tan^2\theta \approx T_C/T_P$ one estimates $\theta \approx 1$ rad. The nonmonotonic behavior of the curves in Fig. 1(b) follows qualitatively the dependence of $\sigma_{xy}(B)$ expected from the Drude model, in agreement with Eq. (1): in low magnetic fields the Faraday rotation increases linearly with B, achieves a maximum at $\mu B/c \approx 1$, and then decreases inversely proportional to B.

The thin sample ($L = 70$ nm) shows similar behavior, but the values of T_C/T_P are significantly smaller because of the smaller sample thickness [Fig. 1(b)]. We find $T_C/T_P = 0.07$ at the maximum (at $B \approx 1$ T), yielding a Faraday rotation $\theta \sim 0.25$ rad. This is actually an astonishingly large number: because of the 70 nm thickness, it corresponds to a very large Verdet constant $\mathcal{V} = 3 \times 10^6$ rad T^{-1} m^{-1}.

We further find that the Faraday effect in HgTe is strongly temperature dependent, it is very weak at liquid Helium temperatures ($\theta \lesssim 1$ mrad) and increases with temperature to very significant values at RT [Fig. 1(c)]. This correlates well with thermally activated conductivity in HgTe, as summarized in Fig. 2. First, we measure the transmission spectrum of a reference CdTe substrate [Fig. 2(a)]. The spectrum shows pronounced Fabry-Perot interference which is nearly independent of temperature. From fitting this data we find the dielectric constant of the substrate: $\varepsilon_{\mathrm{CdTe}} = 9.9$. We find no imaginary part to this quantity, $\mathrm{Im}(\varepsilon_{\mathrm{CdTe}}) \approx 0$, implying that there is no free-carrier absorption in the CdTe substrates and $\sigma_0 \approx 0$. This result is expected, as the band gap of CdTe ($E_g = 1.5$ eV) is much larger than $k_BT = 26$ meV at RT and, therefore, thermally activated carriers can be neglected.

The behavior in HgTe is qualitatively different. This material has an inverted band structure: due to a relativistic correction to the Γ_6 state that derives from Hg-like s-type orbitals, its energy is reduced to below that of the Te-derived p-like Γ_8 band. The light-hole (LH) states of the Γ_8 band now show "conductionlike" behavior and the heavy hole (HH) states in the Γ_8 band show "valencelike" behavior [Fig. 2(b)]. Without strain, the band gap in bulk HgTe is exactly zero, $E_g = 0$ eV. Therefore, the number of activated carriers increases significantly with temperature, even at low temperatures.

This picture is indeed confirmed by the transmission spectra of the HgTe/CdTe epilayers in Fig. 2(c). Here, we observe that the amplitude of the Fabry-Perot interference decreases with temperature and becomes spectrally dependent due to free-carrier absorption in the HgTe layer. This behavior can be modeled well, as shown by solid lines in Fig. 2(c). In the modeling, we assume $\varepsilon_{\mathrm{CdTe}}$ as obtained from the reference CdTe substrate and assume Drude behavior for the free carriers in the HgTe layer. The 2D conductivity $G_0 = \sigma_0 L$ obtained from these fits is plotted in Fig. 2(d) as a function of temperature. We emphasize that, while both electrons and holes are thermally excited, the dominant contribution to the conductivity comes from the conduction band electrons because $m_{LH} \ll m_{HH}$. We have also confirmed this experimentally by measuring the effective mass of the free carriers, as will be discussed later.

In order to obtain more information on the transport characteristics of the free carriers in our samples—this includes carrier concentration N, mobility μ, effective mass m, as well as Faraday rotation θ and Faraday ellipticity η—we have measured the transmission amplitude $|t|$ and phase shift ϕ of the transmitted THz radiation [9].

Experimental data for the 70 nm-thick HgTe layer are shown in Fig. 3. The transmission amplitude measured with parallel polarizers $|t_P|$ shows a W-like behavior as a function of magnetic field [Figs. 3(a) and 3(b)]. The dips in these W-shaped curves correspond to occurrence of the cyclotron resonance (CR) when the frequency ω of the THz radiation equals the cyclotron frequency $\Omega_c = eB/mc$. From these data we find the cyclotron mass in

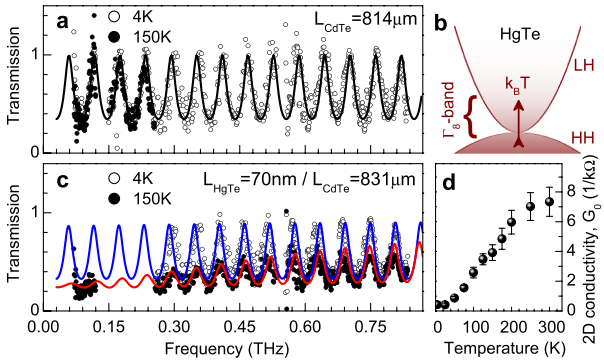

FIG. 2 (color online). *Transmission spectra and optical conductivity.* (a) Transmission spectra of a reference CdTe (814 μm) substrate at different temperatures. (b) Sketch of the dispersion of light-hole (LH) and heavy-hole (HH) bands of the Γ_8 doublet. The arrow indicates thermal excitation of electron-hole pairs. (c) Transmission spectra of the 70 nm-thick HgTe epilayer sample at different temperatures. (d) 2D optical conductivity $G_0 = \sigma_0 L$ of HgTe as a function of temperature. The lines in (a) and (c) result from a model calculation (see text for details).

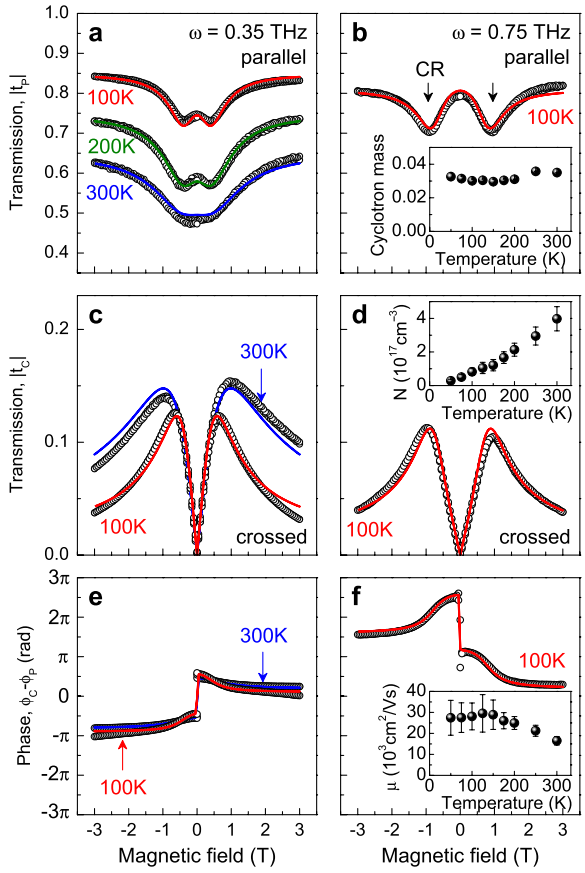

FIG. 3 (color online). *Transmission amplitude and phase shift of the THz radiation in a 70 nm-thick HgTe layer.* (a) Transmission amplitude for parallel polarizers detected at different temperatures at a frequency of 0.35 THz. (b) Transmission amplitude for parallel polarizers detected at $T = 100$ K at a frequency of 0.75 THz. The arrows indicate cyclotron resonance (CR). Inset: cyclotron mass as a function of temperature. (c) Transmission amplitude for crossed polarizers detected at different temperatures at a frequency of 0.35 THz. (d) Transmission amplitude for crossed polarizers detected at $T = 100$ K at a frequency of 0.75 THz. Inset: electron concentration as a function of temperature. (e) Phase difference between parallel and crossed polarization detected at different temperatures at a frequency of 0.35 THz. (f) Phase difference between parallel and crossed polarization detected at $T = 100$ K at a frequency of 0.75 THz. Inset: mobility as a function of temperature. Lines in all panels correspond to the model calculation (see text for details).

HgTe. It slightly varies with temperature [the inset of Fig. 3(b)] and at 100 K is $m = 0.030m_0$, which corresponds to the LH mass [11].

The transmission amplitude in crossed polarizers $|t_C|$ as a function of magnetic field is presented in Figs. 3(c) and 3(d). In low fields $|t_C| \propto |B|$, with a slope that is nearly independent of temperature and decreases with frequency. We have also measured the absolute value of the phase shift (i.e., the optical thickness of the sample) for parallel ϕ_P and crossed polarizers ϕ_C. Figures 3(e) and 3(f) show the phase difference $\phi_C - \phi_P$ for various temperatures and frequencies. The jump in the vicinity $B = 0$ T implies that the Faraday rotation and ellipticity change sign.

The experimental data can be fitted well within a Drude model for the free carriers. The components of the conductivity tensor $\sigma(\omega)$ can be written as [6]

$$\sigma_{xx}(\omega) = \sigma_{yy}(\omega) = \frac{1 - i\omega\tau}{(1 - i\omega\tau)^2 + (\Omega_c\tau)^2}\sigma_0,$$
$$\sigma_{xy}(\omega) = -\sigma_{yx}(\omega) = \frac{\Omega_c\tau}{(1 - i\omega\tau)^2 + (\Omega_c\tau)^2}\sigma_0. \quad (2)$$

The transmission spectra can then be calculated using the transfer matrix formalism [12] (see also supplementary material [9]). For each temperature we simultaneously fit the field dependencies of $|t_P|$, ϕ_P, $|t_C|$, ϕ_C using N, m, and μ as the only fitting parameters. The results of such a fitting procedure are shown as the solid lines in Fig. 3 [see also Figs. 1 and 2], and a very good agreement with experimental data is achieved.

The temperature dependence of the electron concentration in the LH conduction band obtained from these fits is shown in the inset of Fig. 3(d). As expected for a zero-band semiconductor, the carrier density increases significantly with temperature and at RT we have $N = 4 \times 10^{17}$ cm^{-3}. We also find that the mobility μ decreases with temperature, presumably due to phonon scattering [cf. the inset of Fig. 4(f)]. But even at RT μ remains rather high (1.6×10^4 cm^2 V^{-1} s^{-1}). In comparison, typical mobilities in Si at RT are at least an order of magnitude smaller [13].

We now discuss the Faraday effect, which in general can be characterized by the Faraday rotation θ and the Faraday ellipticity η [cf. Figure 4(d)]. The values of θ and η can be directly calculated from the measured transmission amplitudes and phases of the THz radiation [9], and the results for θ and η are shown in Figs. 4(c) and 4(d), respectively. Both curves are antisymmetric with respect to the magnetic field. In the 1 μm-thick sample θ increases linearly up to $B = 0.6$ T. The large slope of 1.3 rad/T suggests a potential for application as a THz polarization modulator. Furthermore, in higher magnetic fields the Faraday rotation decreases much slower than the Faraday ellipticity. At $B = 3$ T we measure $\theta \approx \pi/4$ and as $\eta \ll \theta$, the HgTe layer at this field could be used as a Faraday isolator for THz radiation.

As we already mention above, the large Faraday effect in HgTe is caused by high electron mobility. In order to find the optimal conditions for a given carrier mobility we have calculated how θ depends on frequency and conductivity (or electron concentration). Figure 4(b) shows calculated $\theta(B)$ scans for different frequencies for the 1 μm-thick sample. We find that the maximum rotation oscillates around $\pi/4$, and that for higher THz frequency ω one needs a larger magnetic field to reach this maximum. This is also evident from the theoretical curves (drawn lines) in Fig. 4(e) that give the frequency dependence of the Faraday rotation for both samples at a fixed field. For the 1 μm-thick sample, $\theta_{B=0.6\,\mathrm{T}}$ decreases by an order of

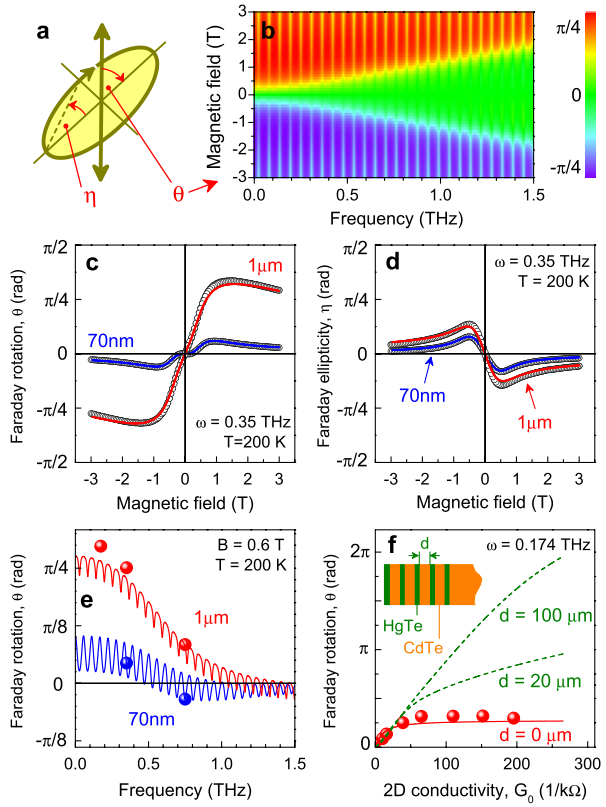

FIG. 4 (color online). *Faraday rotation θ and Faraday ellipticity η as a function of frequency and conductivity.* (a) Definition of θ and η. The vertical double arrow indicates the linear polarization of the incoming radiation, and the ellipse stands for the elliptical polarization of the transmitted radiation. The orientation of this ellipse in the plane is determined by the angles θ and η. (b) Calculated evolution of $\theta(B)$ scans with frequency in the 1 μm-thick sample, $T = 200$ K. Experimental Faraday rotation, (c) and Faraday ellipticity, (d) as a function of magnetic field in both samples. (e) Faraday rotation as a function of frequency at $B = 0.6$ T in both samples. (f) Faraday rotation as a function of 2D conductivity at $\omega = 0.174$ THz and $B = 0.6$ T in a single HgTe layer ($d = 0$ μm) and a HgTe/CdTe periodic structure (shown in the inset). Experimental points are obtained from the temperature dependencies of the Faraday rotation $\theta(T)$ and conductivity $G_0(T)$.

magnitude when ω increases from 0.2 THz to 1.5 THz. The oscillations of θ with frequency ω—which are more pronounced in the thin sample—are caused by multiple reflections in the CdTe substrate.

For further modeling, it is useful to turn to a two-dimensional (2D) sheet description of the Drude gas in our structures. From the conductivity $\sigma = 1900\ \Omega^{-1}\,\mathrm{cm}^{-1}$ of the 1 μm-thick sample at $T = 200$ K, we can calculate a skin depth $\delta = c/\sqrt{2\pi\sigma\omega} \sim 2$ μm. This is the smallest value for the skin depth encountered in the experiments discussed here, and it is obviously still much larger than the thicknesses of the HgTe layers. We can thus assume a homogeneous field penetration and indeed model the Drude gas as a 2D sheet. Using such a 2D Drude model, we have calculated $\theta_{B=0.6\,\mathrm{T}}$ as a function of sheet conductivity $G_0 = \sigma_0 L$, using the mobility as measured at $T = 200$ K [the solid line in Fig. 4(f)]. We find that the Faraday rotation increases linearly with sheet conductivity at low G_0 and saturates at some level for $G_0 > 40\ \mathrm{k}\Omega^{-1}$. The curve is in good agreement with the experimental data [symbols in Fig. 4(f)], which confirms the validity of the sheet model.

An important result that emerges from the calculated graphs in Figs. 4(b) and 4(f) is that the Faraday rotation in our single layer sample never exceeds a maximum value of about 1 rad. As a result, in thick layers θ is no longer proportional to L and, strictly speaking, cannot be characterized by the Verdet constant. In order to enhance the Faraday rotation above this limit we propose to use a periodic HgTe/CdTe heterostructure, as shown schematically in the inset of Fig. 4(f). The structure consists of 10 HgTe layers (which conduct at RT) separated by insulating CdTe layers of thickness d. In Fig. 4(f) we plot $\theta_{B=0.6\,\mathrm{T}}$ as a function of 2D conductivity (dotted lines). Because of constructive interference between the conducting layers, the Faraday rotation is significantly enhanced. For $d = 100$ μm and $G_0 = 265\ \mathrm{k}\Omega^{-1}$ the polarization vector undergoes a complete revolution, i.e., $\theta = 2\pi$.

Summarizing, we have demonstrated that THz spectroscopy is a viable contactless method to study the transport properties of semiconducting and semimetallic thin films. We have found a giant THz Faraday effect in HgTe epitaxial layers, caused by the very high electron mobility at room temperature. Our findings suggest that HgTe has strong potential for practical applications in THz polarimetry.

*astakhov@physik.uni-wuerzburg.de

[1] X. C. Zhang *et al.*, Phys. Rev. B **63**, 245305 (2001).
[2] Y. S. Gui *et al.*, Phys. Rev. B **70**, 115328 (2004).
[3] M. König *et al.*, Science **318**, 766 (2007).
[4] A. B. Villaverde, D. A. Donatti, and D. G. Bozinis, J. Phys. C **11**, L495 (1978).
[5] J. A. Gaj, R. R. Galazka, and M. Nawrocki, Solid State Commun. **25**, 193 (1978).
[6] E. D. Palik and J. K. Furdyna, Rep. Prog. Phys. **33**, 1193 (1970).
[7] G. V. Kozlov and A. A. Volkov, *Millimeter and Submillimeter Wave Spectroscopy of Solids*, edited by G. Grüner (Springer, Berlin, 1998), p. 51.
[8] A. Pimenov *et al.*, J. Phys. Condens. Matter **20**, 434209 (2008).
[9] See supplementary material at http://link.aps.org/supplemental/10.1103/PhysRevLett.106.107404.
[10] C. R. Becker *et al.*, Phys. Status Solidi C **4**, 3382 (2007).
[11] M. Grynberg, R. Le Toullec, and M. Balkanski, Phys. Rev. B **9**, 517 (1974).
[12] D. W. Berreman, J. Opt. Soc. Am. **62**, 502 (1972).
[13] C. Jacoboni *et al.*, Solid State Electron. **20**, 77 (1977).